

**DEVELOPMENT OF AN ENGINEERING MODEL OF BASIN GENERATED
SURFACE WAVES**

Paul G. Somerville, Nancy Collins, Robert Graves, and Arben Pitarka

URS Group, Inc., Pasadena, CA

Abstract

We have developed a modification to the ground motion model of Abrahamson et al. (1997) that takes into account the effects of basin generated surface waves. The main feature of our model is that for response spectral accelerations at periods of 4 and 5 seconds, the Abrahamson and Silva (1997) model for soil sites should be scaled by a factor of 1.65 in order to represent the ground motions on soil sites located within sedimentary basins. Our finding that no scaling of the Abrahamson and Silva (1997) model is required for periods shorter than 4 seconds reflects the fact that most of the deep soil recordings on which that model is based come from sedimentary basins. The fact that our first order model does not have a dependence on distance to the basin edge or the depth of the basin makes it easily applicable in ground motion calculations, especially those for probabilistic seismic hazard analyses, which typically involve the calculation of ground motions from many different scenario earthquakes occurring on a variety of faults surrounding the site. We have identified many second order basin effects that are not quantified in our first order model of basin effects.

Introduction

Many urban regions are situated on deep sediment-filled basins. A basin consists of alluvial deposits and sedimentary rocks that are geologically younger and have lower seismic wave velocities than the underlying rocks upon which they have been deposited. Basins have thickness ranging from a hundred meters to over ten kilometers. It is widely recognized that sedimentary basins have a strong influence on strong ground motions, especially at periods longer than about one second. However, most empirical ground motion models do not explicitly account for these effects.

Current building code criteria including the 1997 UBC (ICBO, 1997) and 2000 NEHRP Provisions (BSSC, 2001) for characterizing site response are based on the average shear wave velocity within the upper 30 meters. In site-specific site response calculations, the response of this soil layer is usually modeled assuming horizontal layering, following the method illustrated on the left side of Figure 1. The wave that enters the layer may resonate in the layer but cannot become trapped within the layer.

At periods longer than one second, seismic waves have wavelengths much longer than 30 meters whose amplitudes are controlled by geological structure having depths of hundreds or thousands of meters, so we expect that seismic velocity structure that is much deeper than 30 meters will influence the amplitudes of long period seismic waves.

In most cases, such as in sedimentary basins, this deeper geological structure is not horizontally layered. If the wave is propagating in the direction in which the basin is thickening and enters the basin through its edge, it can become trapped within the basin if post-critical incidence angles develop. The resulting total internal reflection at the base of the layer is illustrated at the top right of Figure 1.

In the lower part of Figure 1, simple calculations of the basin response are compared with those for the simple horizontal layered model. In each case, a plane wave is incident at an inclined angle from below. The left side of the figure shows the amplification due to impedance contrast effects that occurs on a flat soil layer overlying rock (bottom) relative to the rock response (top). A similar amplification effect is shown for the basin case on the right side of the figure. However, in addition to this amplification, the body wave entering the edge of the basin becomes trapped, generating a surface wave that propagates across the basin.

The development of basin generated surface waves is illustrated in the strong motion recordings of many earthquakes. As an example, the top of Figure 2 shows the location of the fault plane of the 1992 Petrolia earthquake, and the locations of strong motion recording stations in and near the Eel River basin. The direct S wave arrival is shown by the dashed lines in the profiles of filtered velocity waveforms in the bottom of Figure 2. The development of surface waves propagating across the basin is clearly evident in the later arriving phase, indicated by the solid lines. The Eel River basin is about 3 km thick at its deepest point. The surface waves are not present in the recording at station "bunk," which lies outside the basin. The influence of basin structure on recorded ground motions is well explained by basic seismological theory (e.g. Vidale and Helmberger, 1988; Wald and Graves, 1998), and efficient computational procedures have been developed for the modeling of seismic wave propagation in basins (e.g. Graves, 1996; Pitarka, 1999).

Ground Motion Models that Address Basin Structure

Most current empirical ground motion attenuation relations do not distinguish between sites located on shallow alluvium and those located on sedimentary basins. Consequently, these relations may tend to underestimate the ground motions recorded in basins and overestimate those recorded outside basins. However, the influence of basin effects on the amplitudes of strong ground motions has been recognized and incorporated in several ground motion models. These models incorporate basin effects through simplified representations of the basement structure, such as the depth to basement rock beneath the recording site, and the distance from the recording site to the edge of the basin. The depth to basement rock was used as a parameter in the empirical ground motion models of Trifunac and Lee (1979) and Campbell (1997). Lee and Anderson (2000), Field (2002), and Hruby and Beresnev (2002) found that peak accelerations increased with depth to basement in the Los Angeles basin. In the most detailed model for basin effects that has been developed to date (Joyner, 2000), the effect of the basin depends on the distance of the site from the basin edge.

The Joyner (2000) model incorporates differences in ground motion amplitude between the basin edge parallel and basin edge normal components. This model is based on the expectation that there is lateral refraction of surface waves at the basin edge. Alternative models could be

based on the radial and tangential components, or on the average horizontal component. Accordingly, we tested the Joyner (2000) assumption against recorded data as a preliminary step before proceeding with our full analysis of basin effects. We used recordings of the 1999 Hector Mine earthquake in the San Bernardino basin (Wald and Graves, 2003) to analyze the polarization of basin surface waves. These recordings provide clear evidence of lateral refraction of surface waves at the basin edge, which causes the basin waves to be polarized predominantly in the directions parallel to and normal to the edge of the basin, with Love waves predominating on the parallel direction and Rayleigh waves predominating on the normal direction. This is consistent with the assumption made by Joyner (2000). Our analysis also indicates that there can be clear differences in the amplitudes of the basin edge parallel and basin edge normal components. These amplitudes are affected by the relative strength of the incoming waves, which depends on focal mechanism and other factors.

We also used the San Bernardino basin recordings of the 1999 Hector Mine earthquake to analyze the effect of basin depth and distance from basin edge, which are parameters in the Joyner (2000) model, on basin wave amplitudes. The peak velocity increases markedly when the waves enter the San Bernardino basin, and grows in amplitude with increasing distance from the basin edge, even though the distance from the source is increasing. This is due to the trapping of body waves that enter the basin, generating surface waves. There is a clear correlation of peak velocity with basin depth. When depth increases away from the basin edge (i.e. when basin depth and basin edge distance are correlated), this can cause ground motion amplitudes to increase away from the basin edge, and so the basin depth and distance from basin edge do affect basin wave amplitudes, as in the Joyner (2000) model. However, we will show that in most basins this correlation does not hold, apparently due to complexity in basin geometry.

Selection of Strong Motion Recordings for Analysis

This study used recordings from seven earthquake – basin pairs that are listed in Table 1. These include recordings from five different basins, with depths ranging from shallow (a few hundred meters) to deep (up to 9 km), and six different earthquakes, with magnitudes ranging from 6.2 to 7.1. We did not use earthquake – basin pairs in which the earthquake occurred below the basin, such as Whittier Narrows earthquake– Los Angeles basin and Northridge earthquake – San Fernando basin, because this geometry may not lead to the generation of basin waves via the mechanism described in Figure 1.

Table 1. List of Earthquake – Basin Pairs

BASIN		EARTHQUAKE			
Name	Code	Date and Location	Code	M _w	No. of Records
Los Angeles	LA	1971 San Fernando	SF	6.6	21
		1994 Northridge	NR	6.7	48
		1999 Hector Mine	HM	7.1	18
San Bernardino	SB	1999 Hector Mine	HM	7.1	11
San Fernando	SF	1971 San Fernando	SF	6.6	6
Santa Clara	SC	1989 Loma Prieta	LP	7.0	4
Eel River	ER	1992 Cape Mendocino	CM	7.1	8

Development of a Model For Basin Wave Amplitudes

Our approach to developing the ground motion model is to calculate residuals between the recorded ground motions and the predictions of the Abrahamson and Silva (1997) model, and seek correlations between these residuals and basin parameters such as the depth of the basin beneath the recording site, and the distance of the recording site from the edge of the basin. These residuals were first calculated for individual earthquake – basin pairs, and the average values within distance and depth bins were calculated to facilitate the identification of trends of the data. These residuals were then averaged across earthquake - basin pairs to facilitate the identification of general trends.

In Figures 3 and 4, we show residuals averaged over these earthquake – basin pairs for response spectral acceleration having periods of 5, 4, 3, 2, 1.5 and 1 second. The residuals for depth to basement for individual basin – earthquake pairs are quite variable. The Hector Mine earthquake – San Bernardino basin data show the ideal behavior that was described above, in which the peak amplitude increases systematically with increasing depth to basement. Most other earthquake – basin pairs do not show this ideal behavior. The Los Angeles basin residuals from the San Fernando and Hector Mine earthquakes are uniformly high for periods of 4 and 5 seconds, while the residuals for the Northridge earthquake are uniformly low for periods of 3 seconds and longer, especially on the basin edge parallel component. We attribute these systematic differences to differences in closest distance and earthquake source depth, as described further below.

The aggregated residuals for depth to basement, shown in Figure 3, are systematically positive for periods of 4 and 5 seconds, especially on the basin edge parallel component, indicating that the model underpredicts the data. The positive residuals in this period range do not show a systematic dependence on basement depth. The residuals, averaged over the depth range of 0 – 4 km, have an average value of 0.5 natural log units, corresponding to a factor of 1.65. For periods of 2, 1.5 and 1 seconds, the residuals are slightly negative, indicating that the model slightly overpredicts the data.

The residuals for distance from basin edge have patterns that are similar to those depth to basement described above. The residuals for individual basin – earthquake pairs are quite variable. The Hector Mine earthquake – San Bernardino basin data show ideal behavior, in which the peak amplitude increases systematically with increasing distance from the basin edge. Most other earthquake – basin pairs do not show this ideal behavior. The Los Angeles basin residuals from the San Fernando and Hector Mine earthquakes are uniformly high for periods of 4 and 5 seconds, while the residuals for the Northridge earthquake are uniformly low for periods of 3 seconds and longer, especially on the basin edge parallel component. We attribute these systematic differences to differences in closest distance and earthquake source depth, as described further below.

The aggregated residuals for distance to basin edge, shown in Figure 4, are systematically positive for periods of 4 and 5 seconds, especially on the basin edge parallel component, indicating that the model underpredicts the data. The residuals for the basin edge parallel component show little dependence on distance from the basin edge, while the residuals for the

basin edge normal component are small at close distances but grow larger for greater distances. This difference in behavior is described in more detail below. To first order, we model the residuals in this period range as not having a systematic dependence on distance to basin edge, which is most nearly true of the basin edge parallel component. The residuals, averaged over the distance to basin edge range of 0 – 40 km, have an average value of 0.5 natural log units, corresponding to a factor of 1.65. For periods of 2, 1.5 and 1 seconds, the residuals are slightly negative, indicating that the model slightly overpredicts the data.

The residuals for some earthquake – basin pairs are systematically high, while those for others are systematically low. For example, the Los Angeles basin residuals for the San Fernando and Hector Mine earthquakes are uniformly high for periods of 4 and 5 seconds, while the residuals for the Northridge earthquake are uniformly low for periods of 3 seconds and longer. In Table 2, we list these earthquake – basin pairs, indicating whether the residuals are systematically high (+), neutral (o) or low (–), and also indicating whether the earthquake is shallow (significant amount of slip shallower than 5 km) or deep, and whether the earthquake is close (closest distance from most recording stations less than 20 km) or distant.

Table 2. Correlation of Residuals with Earthquake Source Depth and Distance

Earthquake	Source Depth	Basin	Distance	Observed residuals	Predicted residuals
San Fernando	shallow	San Fernando	close	o	o
		Los Angeles	distant	+	+
Northridge	deep	Los Angeles	distant	–	–
Hector Mine	shallow	San Bernardino	distant	+	+
		Los Angeles	distant	+	+
Loma Prieta	deep	Gilroy	close	–	–
Cape Mendocino	deep	Eel River	close	o	–

All of the instances of positive residuals in Table 2 are associated with shallow faulting of distant earthquakes. Shallow faulting on distant sources is associated with shallower incidence (larger incidence angle) of waves entering the basin (Figure 1), making it more likely that postcritical angles will develop inside the basin. We postulate that this is the cause of the positive residuals for shallow distant earthquakes.

In contrast, all of the instances of negative residuals in Table 2 are associated with deep faulting on nearby sources. Deep faulting on nearby sources is associated with steeper incidence (smaller incidence angle) of waves entering the basin (Figure 1), making it less likely that postcritical angles will develop inside the basin. We postulate that this is the cause of the negative residuals for deep nearby earthquakes. We applied this hypothesis related to incidence angle to predict the nature of the residuals that are expected in each earthquake – basin pair in Table 2, and show the prediction next to the observed residuals. In each case, the hypothesis is consistent with the observed residual.

We can test the separate influences of distance and depth in the following way. The shallow faulting San Fernando earthquake was recorded in both the San Fernando basin and the Los Angeles basin. The Los Angeles basin residuals are positive, while the San Fernando basin residuals are neutral. We attribute this to the shallower angle of incidence for waves entering the Los Angeles basin than the San Fernando basin, due to the larger distance of the San Fernando earthquake.

Ground motions from both the shallow San Fernando earthquake and the deep Northridge earthquake were recorded in the Los Angeles basin, at comparable distances. The San Fernando earthquake residuals are positive, and the Northridge earthquake residuals are negative. We attribute this to the shallower angle of incidence for waves entering the Los Angeles basin from the San Fernando earthquake compared with the Northridge earthquake, due to the shallower depth of the San Fernando earthquake.

Our hypothesis is consistent with the trend of increasingly positive residuals with increasing distance, as measured in two ways. In Figure 5, the distance measure is the closest distance to the recording site, including both the segment of the path outside the basin and the segment of the path inside the basin. In Figure 6, the distance measure is the distance from the epicenter to the basin edge, including only the segment of the path outside the basin. For both distance measures, the residuals for periods of 4 and 5 seconds increase with increasing distance, consistent with our hypothesis that the incidence angle controls the likelihood that basin generated surface waves will become trapped, causing positive residuals.

Discussion of Results

Basin Adjustment Factors for the Abrahamson and Silva (1997) Model

To a first approximation, the ground motions recorded in basins are a factor of 1.65 stronger for periods of 4 and 5 seconds than predicted by the Abrahamson and Silva (1997) ground motion model. At periods of 3 seconds and less, no adjustment factor is required; if anything, the ground motions at periods of 1, 1.5 and 2 seconds in this model overpredicts the data. We consider this result to be consistent with the composition of the strong motion data set from which the Abrahamson and Silva (1997) model is derived. Recent large earthquakes that have numerous recordings in basins, such as the 1992 Cape Mendocino, 1992 Landers, and 1994 Northridge earthquakes, are included in the model. The recordings are all from sites with more than 20 meters of soil over bedrock. These deep soil sites are likely to be influenced by surface waves, at least for periods of a few seconds, even if they are not located on deep basins, and so their ground motions on average are adequately predicted by the Abrahamson and Silva (1997) model. However, only those sites located on deep basins are likely to be influenced by basin waves having periods of 4 and 5 seconds, so these ground motions on average are underpredicted by the Abrahamson and Silva (1997) model. In this respect, our model is compatible with the model of Joyner (2000), in which the adjustment factors for the Abrahamson and Silva (1997) model are large only for periods of 4 and 5 seconds.

Averaged over all recordings of all earthquakes, the residuals do not have a strong dependence on distance from the basin edge and on the depth of the basin at the site. Accordingly, we consider that, to a first approximation, it is sufficient to apply the adjustment factors without consideration of these parameters. This considerably simplifies the application of the adjustment factors to the prediction of strong ground motion, compared with the Joyner (2000) model, especially in a probabilistic seismic hazard calculation that addresses a large number of earthquakes occurring at various locations around the basin site. However, there are trends in the residuals that pertain to particular conditions that could be addressed in the calculation of ground motions for specific earthquake scenarios. We address these conditions in the following paragraphs.

Correlation of Basin Wave Amplitude with Distance to Basin Edge and Basin Depth in Simple Basins

In simple basins, in which the basin thickens smoothly from the basin edge, there is a clear increase of basin wave amplitude with increasing distance from the basin edge and with increasing basin depth, when the earthquake source is shallow. The San Bernardino Basin recordings of the 1999 Hector Mine earthquake provide a clear example of this behavior, which is consistent with simple 2D calculations of basin waves in a thickening basin. If a site is located in this kind of situation, the first order model described above will tend to underestimate the ground motions at distances larger than about 10 km from the basin edge.

Differences in Amplitude between Basin Edge Parallel and Normal Components

There are significant differences between the amplitudes of the horizontal component parallel to and perpendicular to the basin edge. This is seen in the residuals for periods of 4 and 5 seconds as a function of distance shown in Figure 4. The residuals for the basin edge parallel component show little dependence on distance from the basin edge, while the residuals for the basin edge normal component are small at close distances but grow larger for greater distances. This behavior is consistent with that in the Joyner (2000) model. In his model, at close distances to the basin edge, the ground motion in the parallel direction is larger than in the perpendicular direction. However, the ground motion in the parallel direction attenuates more rapidly with distance from the basin edge than does the perpendicular component, so at large distances the perpendicular component is larger in his model, with a crossover at about 60 km that varies with period. Our residuals indicate that the basin edge normal component does not grow larger than the basin edge parallel component, contrary to the Joyner (2000) model.

We expect the relative amplitudes of the basin edge parallel and basin edge normal components to be affected by the relative strength of the incoming waves, which depends on focal mechanism and other factors, and on refraction effects. Given the expected complexity of these effects, the observed pattern of relative amplitudes is surprisingly simple. Where there are differences between the two components, which is usually at periods of 3 seconds or longer, the basin edge parallel component is consistently stronger than the basin edge normal component. This is true of individual earthquakes, regardless of focal mechanism, as well as of the data set as a whole.

This result may be attributed to the following cause. For waves with normal incidence on the basin edge, the edge parallel component consists of SH waves that become trapped in the basin as Love waves. These waves are not subject to mode conversion. In contrast, SV waves polarized in the basin edge normal direction would be subject to mode conversion from S to P waves, reducing the strength of the S waves that are transmitted into the basin. This may explain the observation that basin waves on the basin edge parallel component are systematically higher than those on the basin edge normal component.

The residuals between recorded basin ground motions and those computed from the Abrahamson and Silva (1997) model are largest and most consistent for the basin edge parallel component. Positive residuals are also present in the vertical component and to a lesser extent in the basin edge normal component. We recommend that, for simplicity and for conservatism, the distance-independent adjustment factor derived from the basin edge parallel component be applied to all three components of motion.

Dependence of Basin Wave Amplitude on Earthquake Depth

Shallow crustal earthquakes generate significantly stronger basin waves (and larger positive residuals from the Abrahamson and Silva, 1997 model) than do deeper crustal earthquakes. Examples of shallow crustal earthquakes include the 1971 San Fernando, 1992 Landers, and 1999 Hector Mine earthquakes. Examples of deep earthquakes include the 1992 Cape Mendocino and 1994 Northridge earthquakes. This result is expected because shallow earthquakes produce body waves with shallow angles of incidence on the basin edge, enhancing the generation of basin waves, while deep earthquakes produce body waves with steeper angles of incidence on the basin edge, inhibiting the generation of basin waves.

Dependence of Basin Wave Amplitude on Distance of Earthquake from Basin Edge

We have already indicated that basin wave amplitudes in general do not show a strong correlation with distance from the basin edge. However, earthquakes that are located more than about 20 km from the basin edge tend to generate basin waves whose residuals from the Abrahamson and Silva (1997) model are larger than those of closer earthquakes. Examples include the Los Angeles basin recordings of the 1971 San Fernando earthquake, and recordings of the 1999 Hector Mine earthquake in the San Bernardino and Los Angeles basins. We attribute this to the fact that more distant earthquakes produce body waves with shallower angles of incidence on the basin edge, enhancing the generation of basin waves. This explanation is analogous to the one for the effect of earthquake depth given above.

Basin Edge Waves

Large amplification of ground motions occurs when seismic waves enter basins having steep fault-controlled margins. For example, in the 1994 Northridge earthquake, the abrupt deepening of the Los Angeles basin to a depth of several km that occurs at the Santa Monica fault caused the constructive interference of two arrivals: the waves entering the basin from the side, and body waves entering the basin from below, which combined to produce the basin edge wave, as shown schematically in Figure 7.

The bottom left of Figure 8 shows strong motion velocity time histories of the 1994 Northridge earthquake recorded on a profile of stations that begins in the San Fernando Valley, crosses the Santa Monica mountains and extends into the Los Angeles basin (Graves et al., 1998). The locations of the stations are shown on the map, and a geological cross section across the Santa Monica Mountains and Los Angeles basin (profile K-K') is shown below it. The time histories recorded on rock sites in the Santa Monica Mountains (stations encr and spcn) are brief, and are dominated by direct body waves. In contrast, the time histories recorded in the Los Angeles basin (stations uclg and lacn) have much larger amplitudes and longer durations. These large waves consist of surface waves that have become trapped in the Los Angeles basin.

South of the Santa Monica fault, at station smch, even greater amplification occurs where the basin suddenly deepens across the fault. The large long period ground motions recorded at this station are due to the basin edge effect, which is illustrated schematically in Figure 7. The basin edge effect is confined to a zone that is on the order of a few km wide, lying south of the Santa Monica fault. To the south of this zone, the surface wave field resumes its normal development. The synthetic seismograms on the bottom right side of the figure, calculated using the basin structure, reproduce the features of the recorded waves. Much of the damage in the Los Angeles basin during the Northridge earthquake, including the collapse of the I10 freeway and damage to numerous large buildings in Santa Monica and West Los Angeles, is attributable to basin effects and basin edge effects.

A similar basin edge effect was responsible for a zone of extreme damage, located on the edge of the Osaka basin and aligned parallel to the fault through Kobe and adjacent cities on which the 1995 Kobe earthquake occurred (Pitarka et al., 1998). The near-fault ground motions generated by rupture directivity effects in the Kobe earthquake were further amplified by the basin edge effect. This effect was caused by the constructive interference between direct seismic waves that propagated vertically upward through the basin sediments from below, and seismic waves that diffracted at the basin edge and proceeded laterally into the basin (Kawase, 1996; Pitarka et al., 1998). The basin edge effect caused a concentration of damage in a narrow zone running parallel to the causative faults through Kobe and adjacent cities.

In both the Santa Monica and Kobe cases, the basin edge effect is caused by an abrupt lateral contrast in shear wave velocity caused by faulting. Basin edges that have smooth concave bedrock profiles (such as those not controlled by faulting) are not expected to cause basin edge effects. Thus we expect that basin edge effects are not a general feature of basins, but instead are confined to particular kinds of basin edges. In this project, we did not have sufficient recorded data to model the basin edge effect, so the basin edge effect is not included in our model.

Comparison with the Joyner (2000) Model

Our initial approach to developing the basin model was to extend the basin effect adjustment model of Joyner (2000) to shallower basins and to shorter periods, using data from a larger set of earthquakes and strong motion recordings from a larger number of basins. As described above, several important features in the formulation of the Joyner (2000) model were confirmed in the course of our analysis. However, other aspects of the Joyner (2000) model were not confirmed by our analysis. This may be attributable to the fact that our data set consisted of about three times as many recordings, obtained from five different basins instead of just the Los Angeles

basin, and from a larger number of widely recorded earthquakes (five instead of three). In particular, we did not find a systematic dependence of the basin effect on basin depth and distance to the basin edge, although this effect is present for simple basin geometry as exhibited by the San Bernardino Basin recordings of the Hector Mine earthquake. Accordingly, we proceeded to formulate and develop our own model. In Table 3, we compare several features of the basin effects model that we have developed with the one developed by Joyner (2000).

Table 3. Comparison of URS and Joyner (2000) Basin Models

FEATURE	URS Model	Joyner (2000) Model
Number of widely recorded earthquakes analyzed	5: San Fernando, Northridge, Hector Mine, Loma Prieta, Petrolia	3: San Fernando, Northridge, Landers
Number of recordings analyzed	116	41
Number of basins analyzed	5: Los Angeles, San Fernando, San Bernardino, Santa Clara, Eel River	1: Los Angeles Basin
Depth range of basins analyzed	Shallow and Deep	Deep only
Period range analyzed	1 to 5 seconds	0.1 to 5 seconds
Period range of basin effect in model	4 to 5 seconds	3 to 5 seconds
Amplification effect at 4 and 5 seconds period with respect to Abrahamson and Silva (1997) model	1.65	Typically 2 or more; increases with distance to basin edge and with period; also depends on component.
Dependence on distance from basin edge	Considered, but no systematic effect in basic model	Included in model
Dependence on basin depth	Considered, but no systematic effect in basic model	Not considered
Dependence on distance from basin edge and depth for simple basin	Recognized in data; not included in model	Distance effect included in model as a general effect
Different effects for basin edge normal/basin edge parallel components	Recognized in data; not included in model	Included in model
Dependence on earthquake source depth	Recognized in data; not included in model	Not considered
Dependence on distance of earthquake from basin edge	Recognized in data; not included in model	Not considered

Conclusions

We have developed a modification to the ground motion model of Abrahamson and Silva (1997) that takes into account the effects of basin generated surface waves. Several important features in the formulation of the Joyner (2000) model were confirmed in the course of our analysis. Other aspects of the Joyner (2000) model, in particular the dependence of ground motion amplitude on basin depth and distance from basin edge, were found apply to some of the data but not to the data set as a whole. The features of our model are summarized and compared with the Joyner (2000) model in Table 3.

The main feature of our model is that for response spectral accelerations at periods of 4 and 5 seconds, the Abrahamson and Silva (1997) model for soil sites should be scaled by a factor of 1.65 in order to represent the ground motions on soil sites located within sedimentary basins.

The fact that our first order model does not have a dependence on distance to the basin edge or the depth of the basin makes it easy to apply in ground motion calculations, especially those for probabilistic seismic hazard analyses, which typically involve the calculation of ground motions from many different scenario earthquakes occurring on a variety of faults surrounding the site. This makes our model much simpler to apply than the Joyner (2000) model, for which the distance from the source to the basin edge and the distance from the basin edge to the site must be calculated for each earthquake scenario.

For the calculation of ground motions for individual scenario earthquakes at basin sites, we have identified a number of features that can influence the ground motions in addition to the effects of the first order model. These features, listed in Table 3, include the correlation of amplitude with distance to basin edge and depth of basin in simple basins, the difference between basin edge normal and parallel components, the depth of the earthquake, the distance of the earthquake from the basin edge, and basin edge effects. These effects are likely to depend on the location of the site within the basin, not just on the basin depth and the distance from the basin edge, and thus may best be treated using zonation of the basin rather than through the development of simple rules based on basin depth and the distance from the basin edge. The effects at a given location are also likely to depend on the location of the earthquake (Olsen, 2000), so that the zonation for basin effects needs to consider the variability caused by different earthquake locations.

References

Abrahamson, N.A. and W.J. Silva (1997). Empirical response spectral attenuation relations for shallow crustal earthquakes. *Seism. Res. Lett.* 68, 94-127.

Building Seismic Safety Council (2001). NEHRP Recommended Provisions for Seismic Regulations for New Buildings and Other Structures, 2000 Edition. FEMA 368.

Campbell, K.W. (1997). Empirical near-source attenuation relationships for horizontal and vertical components of peak ground acceleration, peak ground velocity, and pseudo-absolute acceleration response spectra. *Seism. Res. Lett.* 68, 154-179.

Field, E.H. (2000). A modified ground motion attenuation relationship for Southern California that accounts for detailed site classification and a basin depth effect. *BSSA*, 90, S209-S221.

Graves, R.W. and D.J. Wald (2003). Observed and simulated ground motions in the San Bernardino basin region for the Hector Mines earthquake. *Bull. Seism. Soc. Am.*, 93, in press.

Graves, R. W., A. Pitarka, and P. G. Somerville (1998). Ground motion amplification in the Santa Monica area: effects of shallow basin edge structure. *Bull. Seism. Soc. Am.*, 88, 1258-1276.

Graves, R.W. (1996). Simulating seismic wave propagation in 3D elastic media using staggered grid finite differences, *Bull. Seism. Soc. Am.*, 86, 1091-1106.

Hruby, C. and I. Beresnev (2002). Empirical corrections for basin effects in stochastic ground motion prediction. *Eos Trans. AGU*, Abstract S12B-1223.

International Conference of Building Officials (1997). Uniform Building Code, 1997 Edition.

Joyner, W.B. (2000). Strong motion from surface waves in deep sedimentary basins. *Bull. Seism. Soc. Am.*, 90, S95-S112.

Kawase, H., The cause of the damage belt in Kobe, the "basin edge effect," constructive interference of the direct S-wave with the basin-induced diffracted/Rayleigh waves. *Seism. Res. Lett.*, 67, No.5, 25-34.

Lee, Y. and J.G. Anderson (2000). Potential for improving ground motion relations in Southern California by incorporating various site parameters. *Bull. Seism. Soc. Am.* 90, S170-S186.

Olsen, K.B. (2000). Site amplification in the Los Angeles Basin from three-dimensional modeling of ground motion. *Bull. Seism. Soc. Am.*, 90, S77-S94.

Pitarka, A. (1999). 3D finite-difference modeling of seismic motion using staggered grid with non-uniform spacing, *Bull. Seism. Soc. Am.*, 89, 54-68.

Pitarka, A., K. Irikura, T. Iwata and H. Sekiguchi (1998). Three-dimensional simulation of the near-fault ground motion for the 1995 Hyogo-ken Nanbu (Kobe), Japan, earthquake. *Bull. Seism. Soc. Am.*, 88, 428-440.

Trifunac, M.D. and V.W. Lee (1979). Dependence of pseudo-relative velocity spectra of strong ground motion acceleration on the depth of sedimentary deposits. *Rept. No. CE79-02*, Dept. of Civil Engineering, University of Southern California, Los Angeles.

Vidale, J.E. and D.V. Helmberger (1988). Elastic finite-difference modeling of the 1971 San Fernando, California earthquake. *Bull. Seism. Soc. Am.*, 78, 122-141.

Wald, D.J. and R.W. Graves (1998). The seismic response of the Los Angeles basin, California. *Bull. Seism. Soc. Am.*, 88, 337-356.

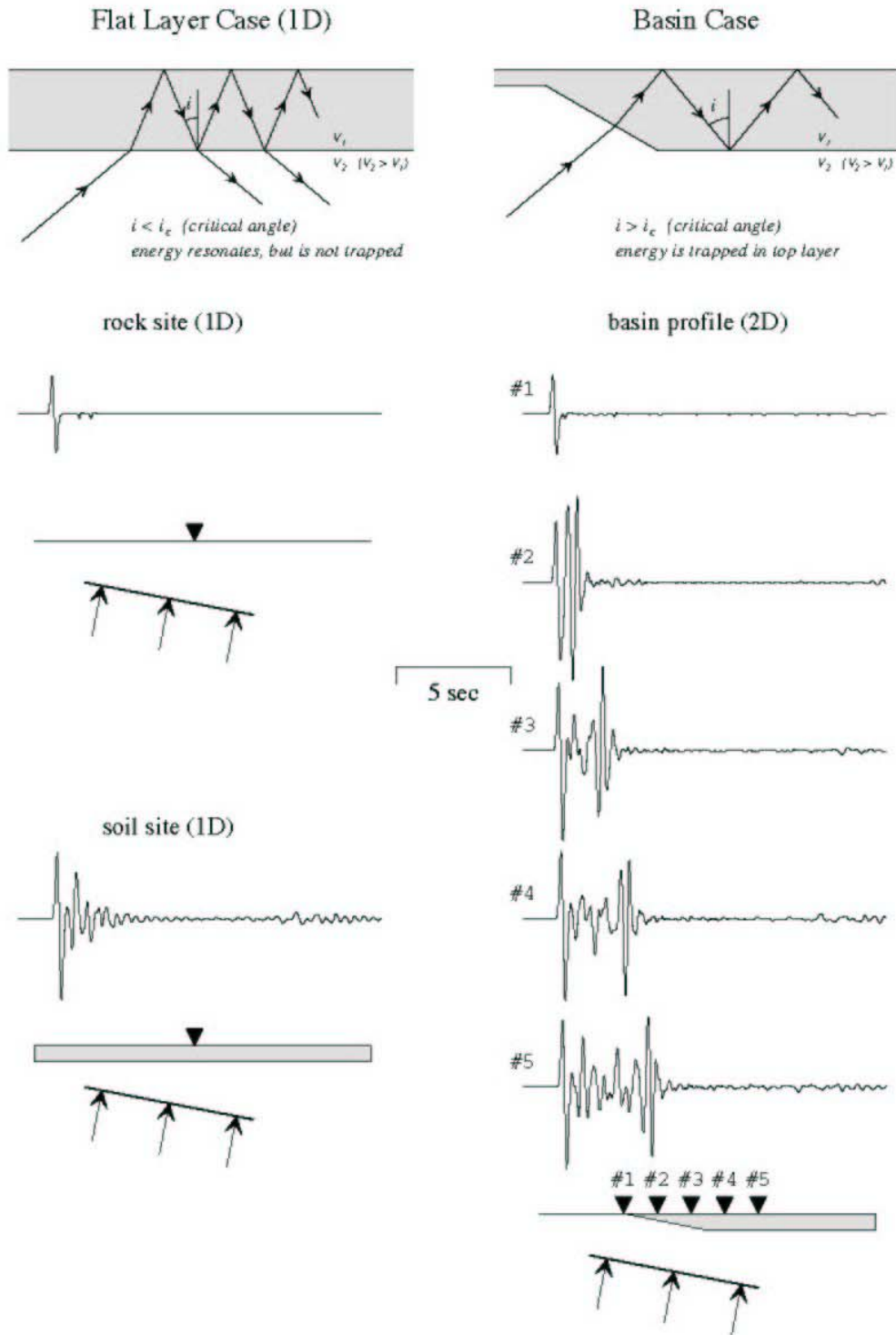


Figure 1. Schematic diagram showing that seismic waves entering a sedimentary layer from below can escape if the layer is flat (left), but can become trapped in the layer, generating a surface wave, if the layer has variable thickness (as in the case of waves entering a basin through its edge). Source: Graves, 1993.

Cape Mendocino Earthquakes

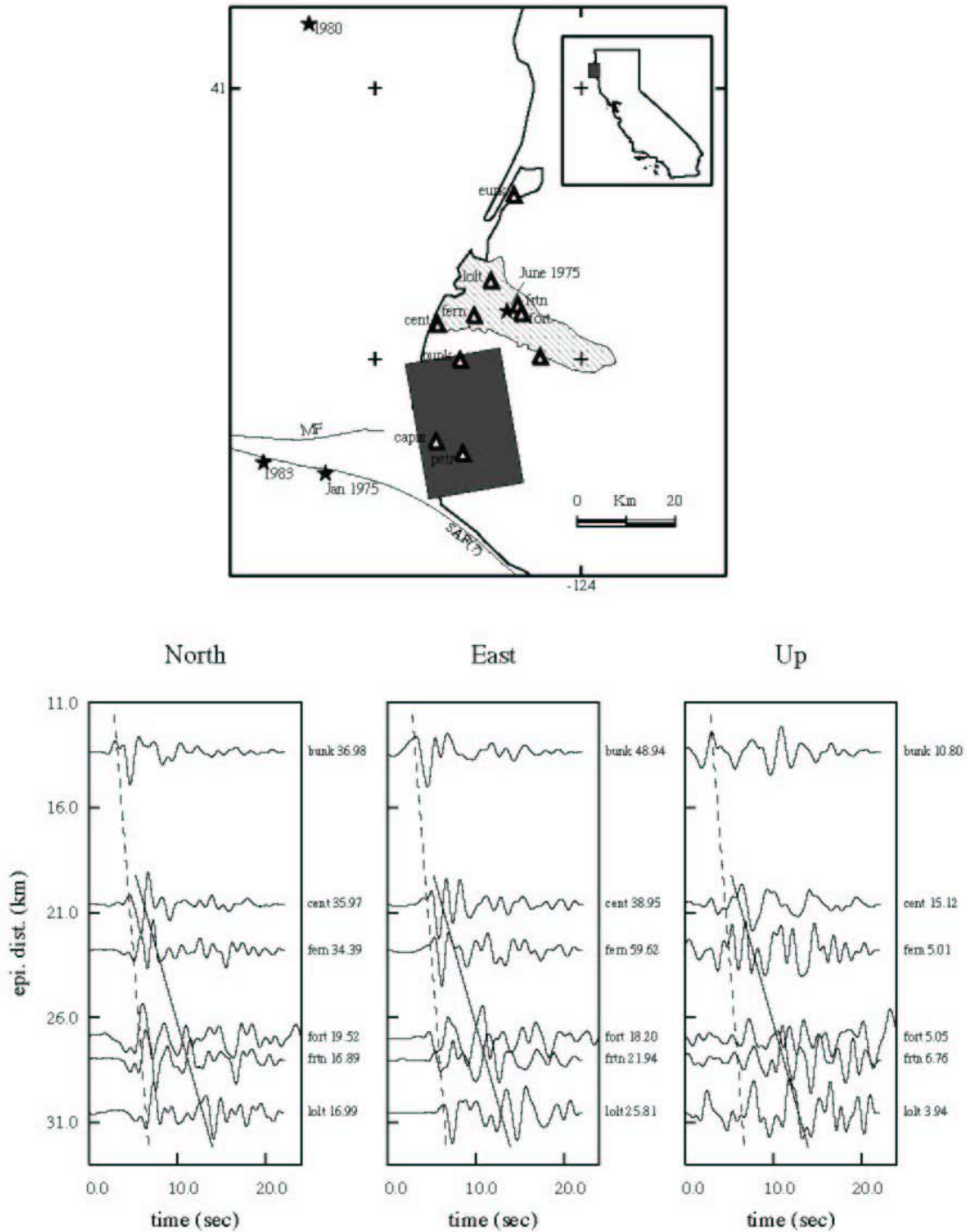


Figure 2. Top: Location of the fault plane of the 1992 Petrolia earthquake, the Eel River basin, and strong motion recording stations. Bottom: Profiles of filtered velocity waveforms recorded across the Eel River basin during the 1992 Petrolia earthquake. The direct S wave arrival is shown by the dashed lines, and the development of surface waves propagating across the basin is clearly evident in the later arriving phase, indicated by the solid lines. Source: Graves, 1994.

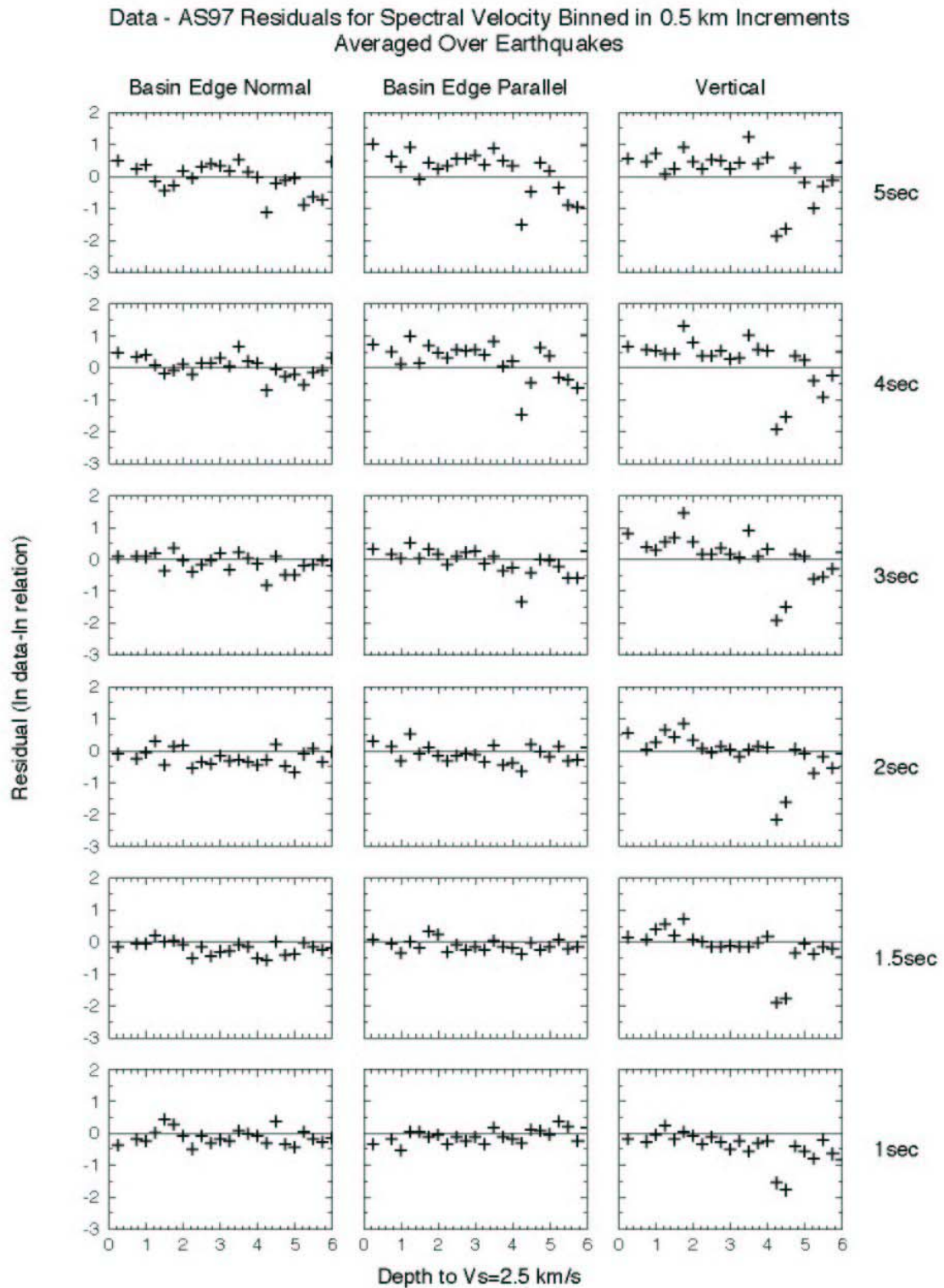


Figure 3. Residuals (data - model) of response spectral velocity of three components of motion recorded on basin sites for a series of periods, as a function of depth to basement. Residuals for individual earthquake - basin pairs, binned at 0.05 km depth intervals have been aggregated.

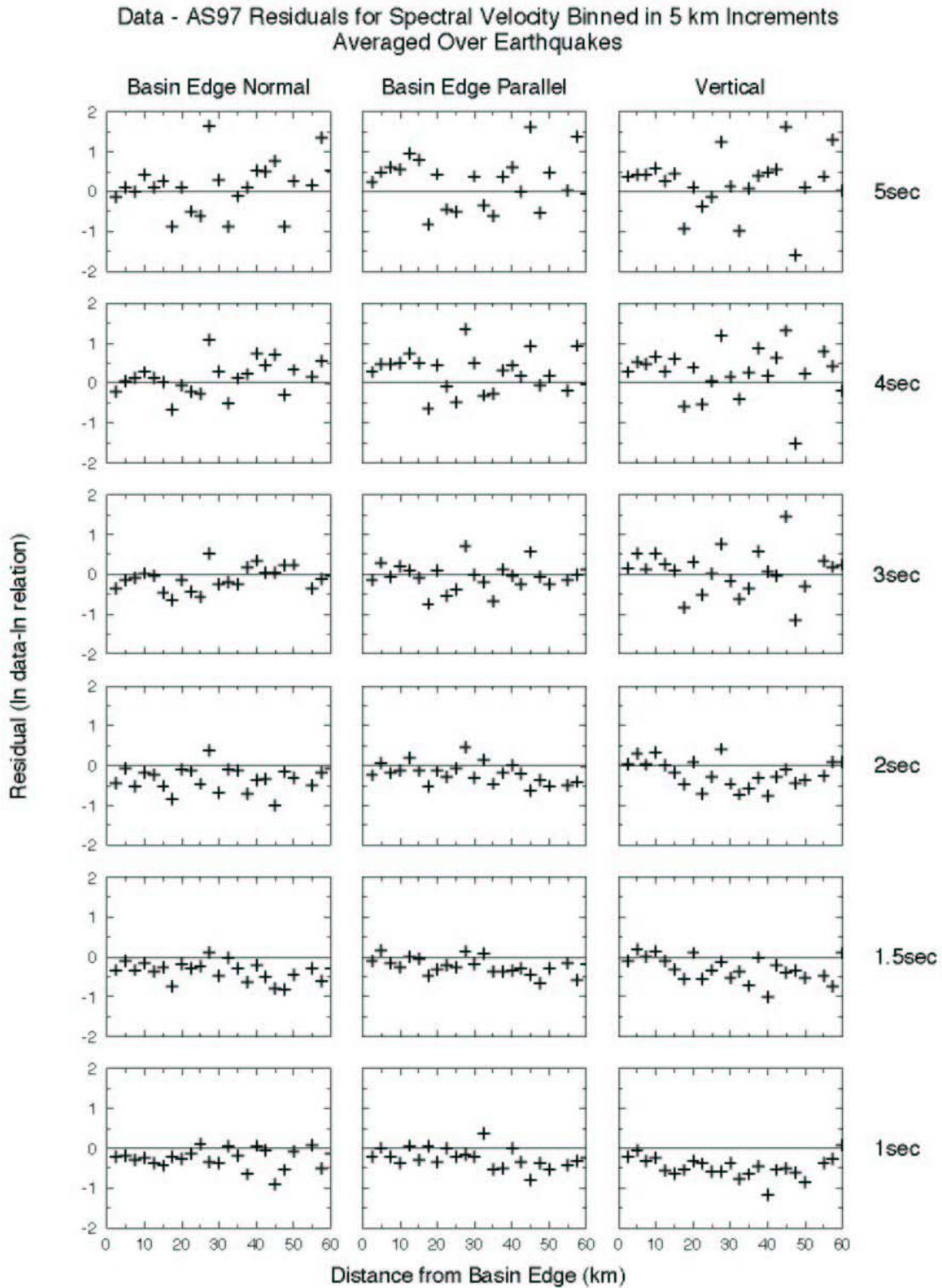


Figure 4. Residuals (data – model) of response spectral velocity of three components of motion recorded on basin sites for a series of periods, as a function of distance from basin edge. Residuals for individual earthquake – basin pairs, binned at 0.5 km distance intervals have been aggregated.

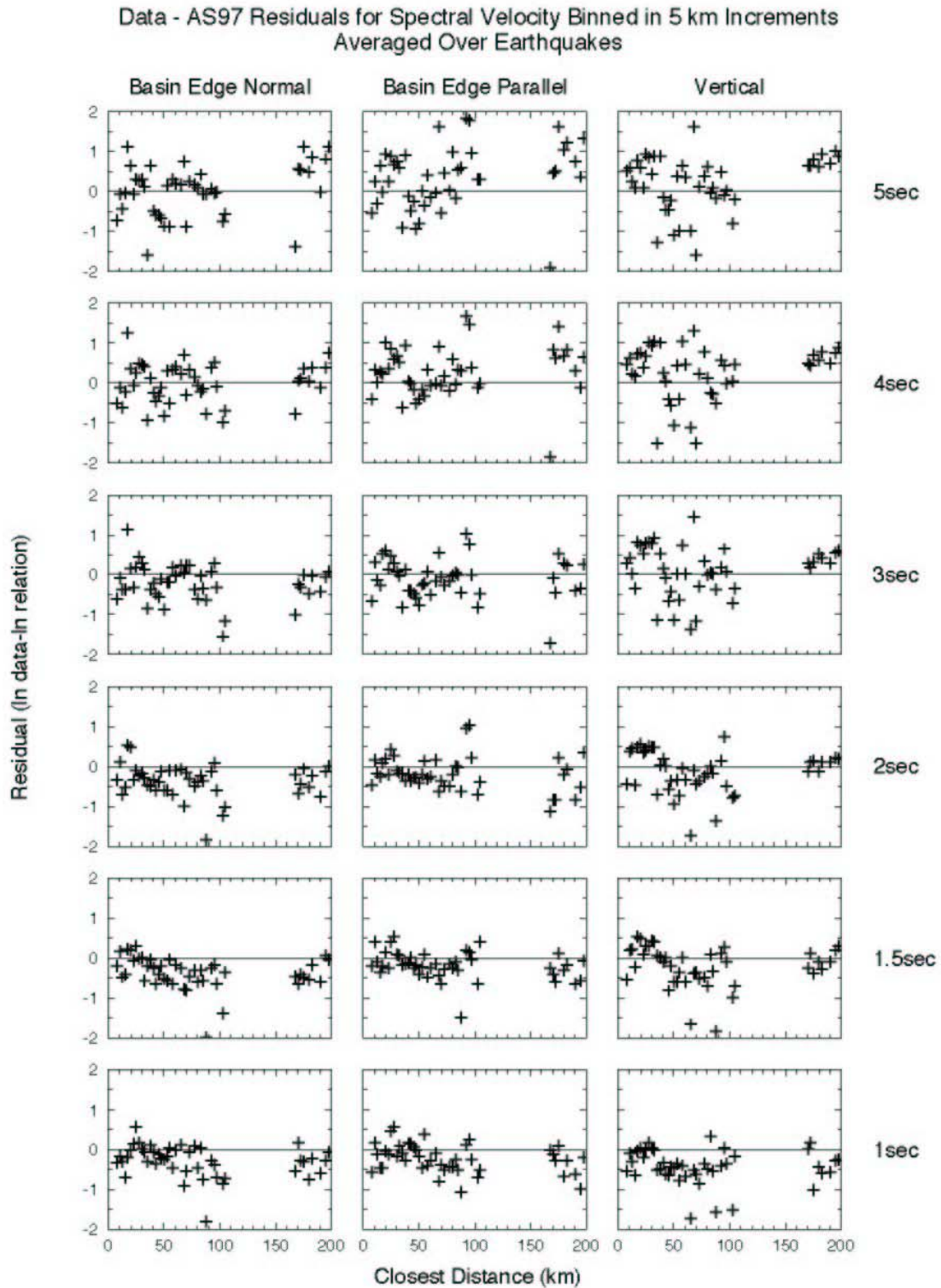


Figure 5. Residuals (data – model) of response spectral velocity of three components of motion recorded on basin sites for a series of periods, as a function of closest distance. Residuals for individual earthquake – basin pairs, binned at 0.5 km distance intervals have been aggregated.

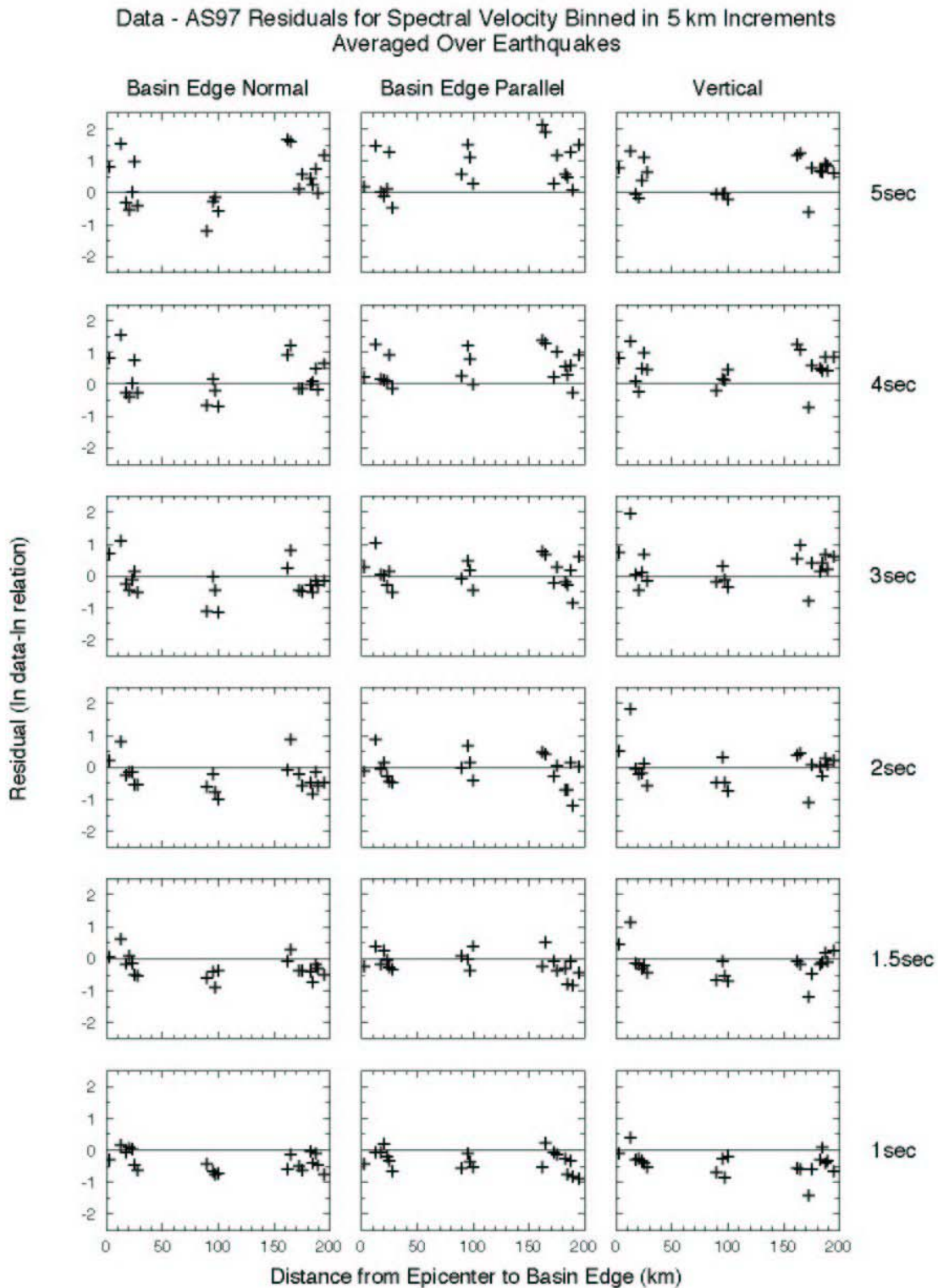


Figure 6. Residuals (data – model) of response spectral velocity of three components of motion recorded on basin sites for a series of periods, as a function of distance from epicenter to basin edge. Residuals for individual earthquake – basin pairs, binned at 0.5 km distance intervals have been aggregated.

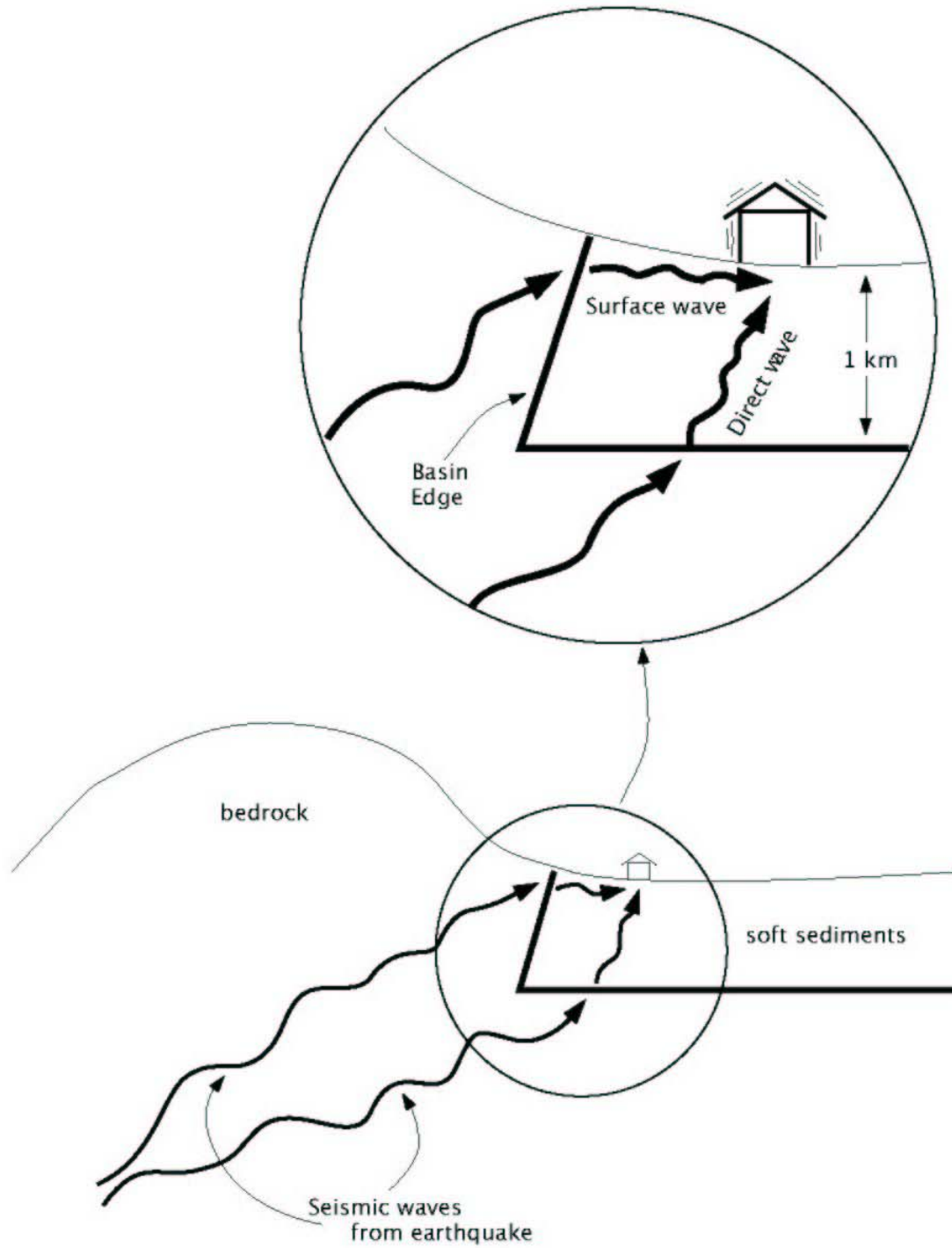


Figure 7. Schematic diagram showing how the basin edge effect is caused by the constructive interference between the direct wave, which travels through the bottom of the basin, and the diffracted wave, which travels through the edge of the basin.

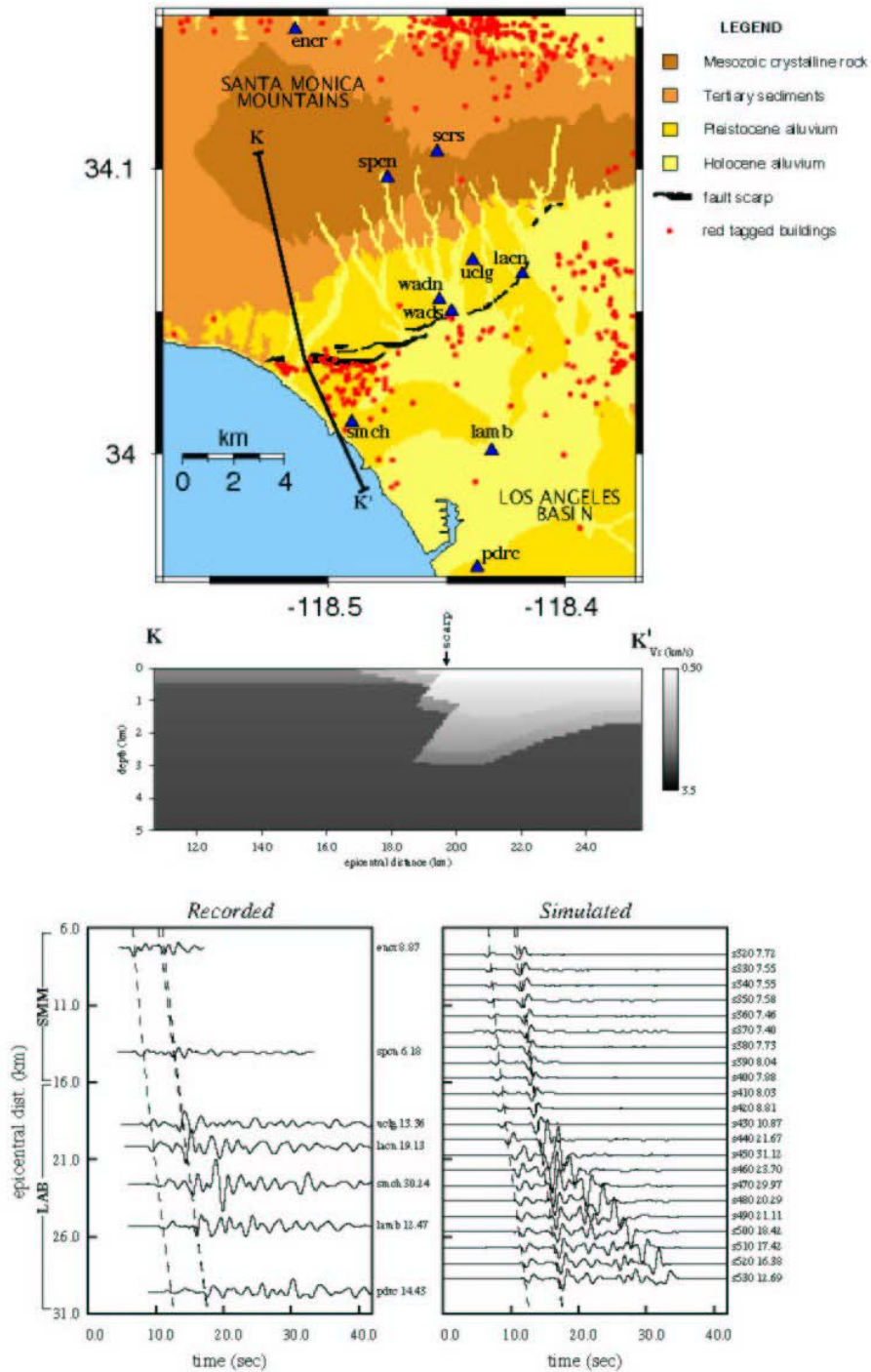


Figure 8. Surface waves generated in the west Los Angeles basin during the 1994 Northridge earthquake. Surface waves were initially trapped in the shallow sediments north of the Santa Monica fault. The abrupt deepening of the Los Angeles basin to a depth of several km that occurs at the Santa Monica fault caused the basin edge wave, manifested in the large long period pulse of motion recorded at Santa Monica. Further south of the Santa Monica fault, the surface waves resumed their normal development. Source: Graves et al., 1998.